VOL. 20, NO. 2-2, 2021, 36-40
www.elektrika.utm.my
ISSN 0128-4428

ELEKTRIKA
Journal of Electrical Engineering

Finite Element Analysis of Silicon Nanowire Array based SAW Gas Sensor

Muhammad Izzudin Ahmad Asri, **Md. Nazibul Hasan**, **Mariatul Rawdhah Ahmad Fua'ad**, **Fatimah Khairiah Abd Hamid**, **Yusri Md Yunos*** and **Mohamed Sultan Mohamed Ali***

School of Electrical Engineering, Universiti Teknologi Malaysia, 81310 UTM Johor Bahru, Johor, Malaysia.

*Corresponding author: yusri@utm.my; sultan_ali@fke.utm.my

Abstract: This work presents the design and finite element analysis of a surface acoustic wave (SAW)-based sensor for the detection of volatile organic compound (VOC) gases. The effect of silicon nanowire array (SiNWA) on a 128° YX-lithium niobate ($LiNbO_3$) substrate for sensing the VOC gases was simulated using COMSOL Multiphysics. The frequency response was investigated in relation to changes in the SiNWA sensitive layer and VOC gas concentration. The resonant frequency of the SAW device was also evaluated, and simulation results were obtained after being exposed to 100ppm concentration of VOC gas. It was determined that the frequency increased, after the sensor was exposed to VOC gases. In general, extending the length of the SiNWA enhances the sensor's sensitivity.

Keywords: COMSOL, SAW gas sensor, SiNWA, VOC gases.

Article History: received 25 May 2021; accepted 12 June 2021; published 15 September 2021.

1. INTRODUCTION

Volatile organic compound (VOC) gases are commonly used in the production of fuels, solvents, compressed aerosols, and other similar compounds. Long-term inhalation of VOC gases has the ability to threaten human health by impeding the central nervous system, causing dizziness and headaches, as well as severe myocardial damage and other disorders [1-3]. Accordingly, highly sensitive analytical techniques such as gas phase sensors, absorption spectroscopy, gas chromatography, and TDLAS detection technology have been used for the accurate quantification of these gases [4-7]. Despite their accuracy and precision, these techniques have some major drawbacks, such as high-power demand, higher costs, and lack of portability. In addition, the utilization of such techniques often requires complex and time-consuming steps, as well as highly skilled operators. These procedures are unable to provide real-time gas exposure information. Consequently, gas sensing devices, which are small, inexpensive, and easy to use, are promising and should be investigated further. The use of micro-electromechanical systems (MEMS) technology in gas sensing applications, is therefore significant. Gas sensors based on SAW have received a lot of attention to detect chemical agents and gases, owing to their small size, rapid responses, portability, and fundamental frequency reliability[8,9].

SAW sensors incorporating nanostructured sensitive material have showed significant improvements in efficiency and sensitivity due to high surface-to-volume ratio, allowing for the design of a compact gas sensor [10-12]. Thus, most of the sensing layer of SAW gas sensor is made of oxide-based materials such as ZnO, TiO_2, graphene oxide (GO), and absorbent polymers [13].

To design and predict the various characteristic parameters of the MEMS sensor, finite element method (FEM) was utilized. For instance, Hercules et al. obtained a high sensitivity for a SAW sensor based, utilizing zinc oxide nanopillars-based sensitive material layer and 128º YX-$LiNbO_3$ piezoelectric substrate [14]. Hasan et al. developed a SAW-based hydrogen sensor with ZnO nanorod, as sensitive materials, and studied the influence of layered and nanostructured sensing layers on surface acoustic wave propagation [15]. Wang et al. theoretically investigated a methane gas sensor utilizing 36º YX-$LiTaO_3$ piezoelectric substrate [16]. They used cryptophane-A coated SiO_2 guided layer in this study and demonstrated exceptional sensitivity and rapid response. In another study, Moustafa et al. performed FEM analysis to detect dichloromethane using SAW sensor, which consisted of polyisobutylene and ZnO as sensing material and substrate, respectively [17]. Nonetheless, the development of novel low-cost sensitive layers and high-performance gas sensors requires further investigation and research.

This study provides the 2-dimensional modeling simulation of a SAW sensor and its performance while various VOC gases are being used. Section 2 discusses the working principle of the SAW sensor as well as performance factors. Section 3 discusses the results and discussion for the detection of various types of VOC gases. Section 4 concludes with a summary of outcomes.

2. WORKING PRINCIPLE AND SENSOR DESIGN

SAW gas sensors are a type of MEMS sensor that detects a physical element via modulating surface acoustic waves. The SAW gas sensor is consisting of a 128º YX-$LiNbO_3$ piezoelectric substrate, interdigital transducers (IDTs), and a sensitive material in the middle of the SAW sensor, as shown in Figure 1(a) [18]. An electrical signal is converted to a surface acoustic wave by the input IDTs, and the surface acoustic wave is converted back to an electrical signal by the output IDTs. An alternating polarity between neighboring IDTs is generated by the sinusoidal electrical input signal to a piezoelectric acoustic wave sensor. This alternating electric field causes compressive strain and alternating tensile regions due to the piezoelectric effect [18]. Consequently, a mechanical wave, regarded as the acoustic wave, is formed at the surface, as depicted in Figure 1(b). Figure 2(a) illustrates the proposed SAW gas sensor geometry, which includes four input and output IDTs, made of aluminum, with a height and width of 2 µm and 50 µm, respectively, and a 100 µm spacing between two electrodes that are placed over a piezoelectric substrate. The sensors operating frequency was set to around 26 MHz and the substrate dimensions were set to 1500 µm × 100 µm. The pitch of the SAW gas sensor was set to 150 µm, while the SiNWA-based sensing layer was developed with a length ranging from 300 nm to 700 nm.

The sensor was simulated in two dimensions with COMSOL Multiphysics, considering its solid mechanics and electrostatics modules. In the parameters section, the sensing layer's properties, including young's modulus, poisons ratio, and relative permittivity, were defined. The young's modulus, relative permittivity and Poison's ratio was set to 160 GPa, 4.5, and 0.22 nu, respectively. The sensor was analyzed based on eigen frequency evaluation. Figure 2(b) shows a cross-section of the mesh analysis model. For this simulation, an extra fine meshing was used to the dimensions of the SiNWA sensing layer. The absorption of gas by the SiNWA was indicated as an increase in the density of the film [1]. Without gas, the density of the SiNWA was 2320 g/m^3. At room temperature and atmospheric pressure, the SAW gas sensor was exposed to 100-5000 ppm of various VOC gases. When a voltage (12 V) was applied to the input electrodes, the piezoelectric effect caused mechanical perturbations on the surface. These acoustic waves propagate along the surface, and when they reach the output electrodes, they generate a direct piezoelectric effect voltage across them. Equations 1, 2, and 3 explain the behavior of a piezoelectric material. The electric flux (D) and stress vector (T) is two significant parameters that affect the operation of the SAW sensor. The following equation calculates stress [15]:

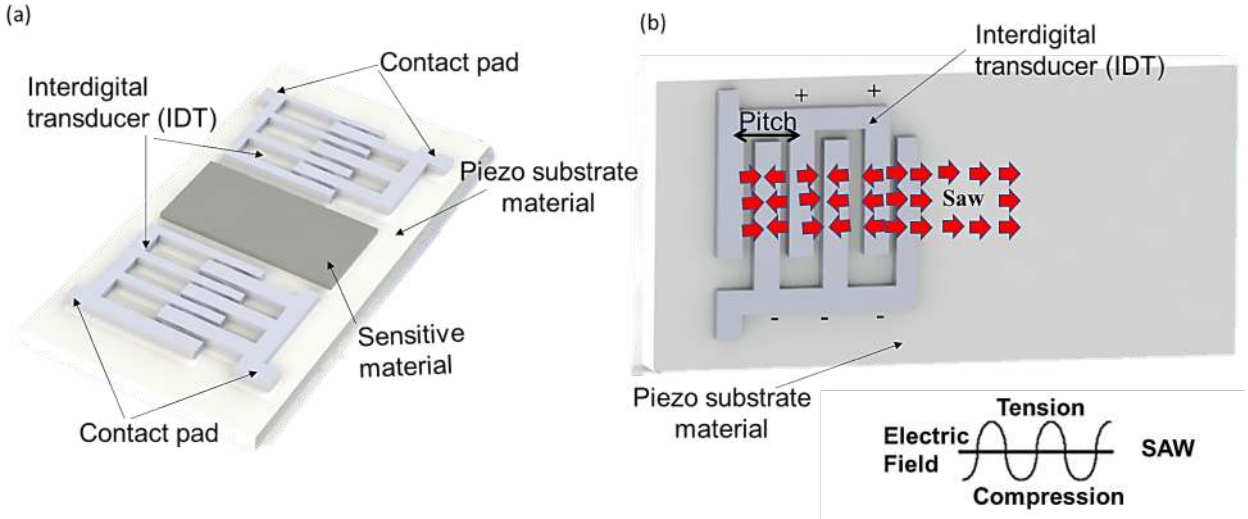

Figure 1. (a) The schematic design and (b) Mechanism of of SAW gas sensor.

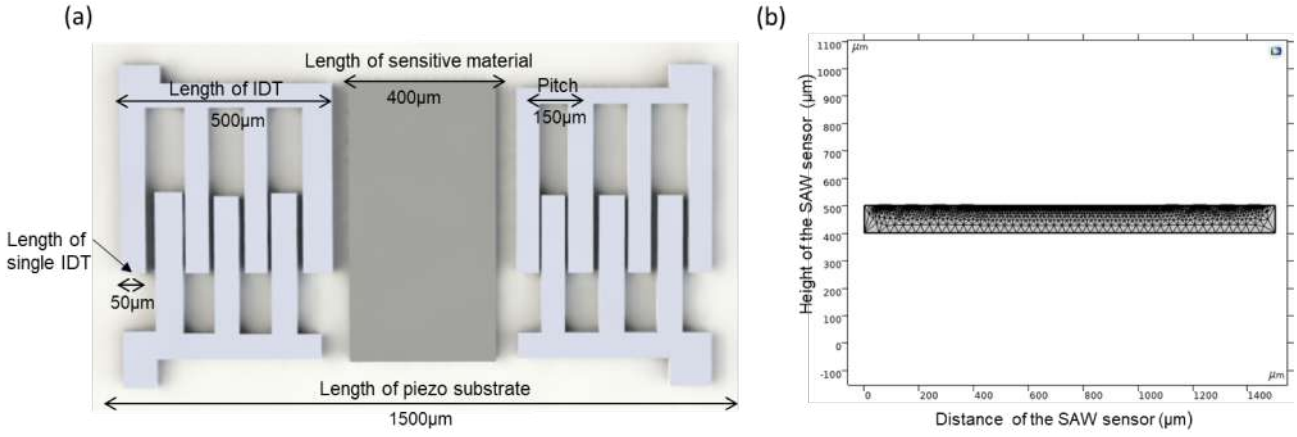

Figure 2. (a) Proposed layer of SAW. (b) Proposed layer of SAW with extra meshed triangular.

$$T = cS - eE \quad (1)$$

where c and S define the elasticity matrix and strain vector, respectively, and e and E are the dielectric matrix and electric field, respectively. For structural mechanics, Equation 1 was used. The electric flux is described as follows [15]:

$$D = e^T S + \varepsilon E \quad (2)$$

where ε is the piezoelectric matrix. The resonance frequency, f_0, of a SAW device, which is determined by the acoustic wave propagation velocity (V_p) in the piezoelectric substrate and the pitch, (p) as follows: [18,19]:

$$f_o = \frac{Vp}{p} \quad (3)$$

The device resonant frequency should be equal to the frequency of the input electrical signal to ensure high efficiency on the SAW device. The frequency range of the acoustic waves it generates is defined by the bandwidth (BW) of the input IDT. To enhance the BW for a SAW sensor, the number of pairs of IDT fingers can be increased. When determining the number of fingers in the IDT, the number of pairs is taken into consideration. A SAW device's BW is defined as follows [18,19]:

$$BW = \frac{2f_0}{N} = \frac{2V_P}{N.p} = \frac{2V_p}{l_{IDT}} \quad (4)$$

where N defines the number of pairs in the IDT and l_{IDT} is the total length of the IDT, respectively. The amplitude at the synchronous frequency can be increased by minimizing the BW, resulting in a more distinct signal, according to Equation 4. The length of the IDT is inversely proportional to the BW.

The fundamental gas sensing mechanism of a surface acoustic wave sensor is based on the principle of the absorption of gas molecules by the sensing layer. Due to gas absorption in the sensing layer, the velocity of the acoustic wave varies, which may be easily detected by the SAW sensor based on the frequency shift. The variation of frequency (Δf) can be defined as:

$$\Delta f = (K_1 + K_2) f_0^2 \sigma \quad (5)$$

where K_1 and K_2 are the coupling constant, f_0^2 and σ are the frequency of the propagation wave and the area density of the formed layer by the absorbed gas, respectively. The wavelength of the surface acoustic wave sensor, which depends on the electrode finger width (h) and p can be defined as [18,19]:

$$\lambda = 2(h + p) \quad (6)$$

In Equations 3, 4, and 6, several parameters can be employed to maximize the performance of the SAW gas sensor. The molar mass ($gmol$) and air partition coefficient (k) of methanol, trichloromethane, dichloromethane, acetonitrile, and acetone VOC gases are shown in Table 1, enabling the partial density of absorbed gas in SiNWA to be determined.

3. RESULT AND DISCUSSION

After meshing and simulating the model, the yielded propagation properties of the SAW device were investigated. The resonant frequency for the sensor is around 26MHz. The lowest Eigen frequency represents series resonance, without being exposed to gas; while the other represents parallel ("anti-") resonance, exposed to gas (Figure 3). The sensor was tested with 100 ppm of acetone, dichloromethane, methanol, acetonitrile and trichloromethane VOC gases. Table 2 summarizes the frequency shift at the surface of the device when exposed to 100 ppm VOC gas at 1 atm and room temperature. As the gases have different partial densities, the resonance frequency thus shifts differently, making it possible to detect each VOC gas. The model showed a maximum response on methanol gas with a higher resonance frequency shift. The resonant SAW mode with a resonant Frequency of 26.047MHz is shown in Figure 3(a). Resonant saw mode occurs due to constructive interference of propagating waves. It is seen that majority

Table 1 Molar mass and air partition coefficient for different VOC gases.

Gas	Molar mass (gmol)	Air partition coefficient (k)
Acetone	58.68	$10^{4.87}$
Dichloromethane	84.93	$10^{4.18}$
Methanol	32.06	$10^{4.38}$
Acetonitrile	41.05	$10^{4.01}$
Trichloromethane	119.38	$10^{4.36}$

Table 2 Frequency shift of various VOC gases.

Gas	Resonance frequency before exposure (MHz)	Resonance frequency after exposure (MHz)	Frequency shift (kHz)
Acetone	26.047	26.059	-12
Methanol	26.047	26.082	-35
Trichloromethane	26.047	26.067	-20
Dichloromethane	26.047	26.075	-28
Acetonitrile	26.047	26.079	-32

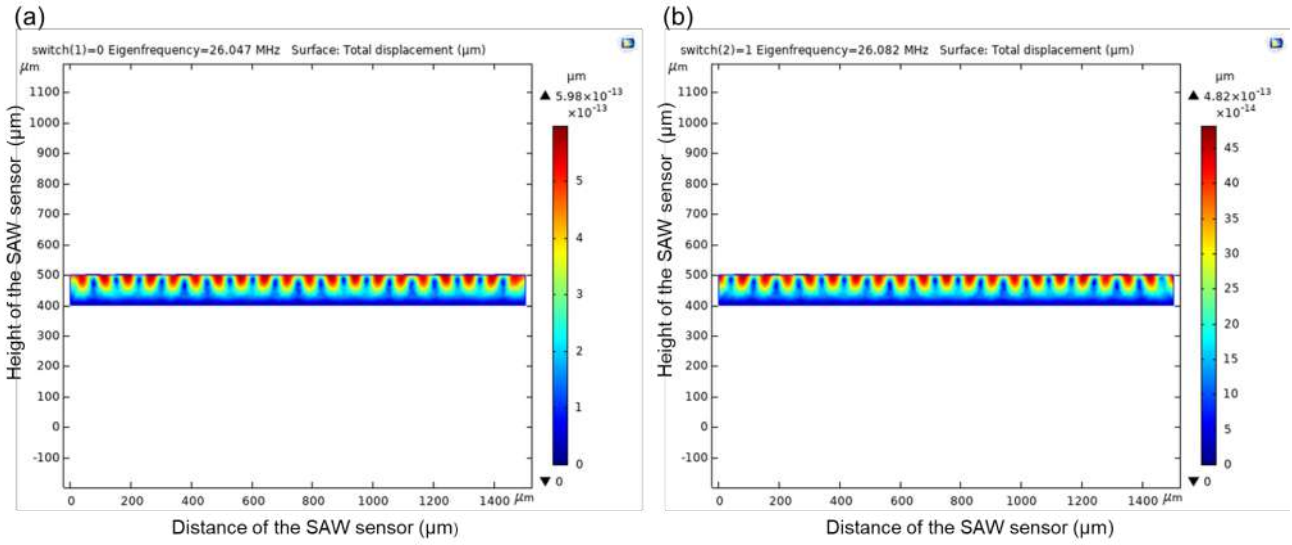

Figure 3. Deformed plot showing (a) SAW resonance mode and (b) SAW anti-resonance mode.

of the saw waves occur at the surface, and the amplitude decreases with the depth of the material. Figure 3(b**)** shows the anti-resonant SAW mode with a resonant frequency of 26.082MHz. The destructive interference of propagating waves causes anti-resonant saw mode to occur. In this simulation, two types of evaluations were performed: frequency shift of the sensor *vs* concentration of gas, and frequency shift *vs* thickness of sensing material.

3.1 Frequency Shift vs Concentration of Gas

As the concentration of VOC gas increases, more gas particles are absorbed at the sensing layer's surface. As shown in Figure 4, the frequency shift is proportional to the concentration of VOC gas. Acetone, dichloromethane, and trichloromethane gases have shown a higher frequency shift compared to other VOC gases in this study. The frequency shift for acetone is 760 kHz when acetone with concentration of 5000 ppm is exposed to SiNWA sensing layer.

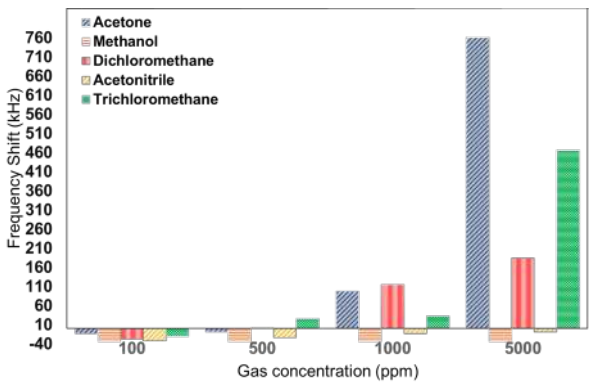

Figure 4 Frequency shift of the sensor *vs* concentration of gas.

3.2 Frequency Shift vs Height of Sensing Material

The height of the sensing layer is an important factor in determining the frequency of SAW sensors. At 100ppm gas concentration, the frequency shift at different sensing layer height was investigated for various VOC gases. Figure 5 depicts the obtained results with varying SiNWAs length ranged between 300 and 700 nm. It can be seen that the frequency resonance enhances with height. This is due to the fact that 700 nm SiNWA has a higher surface-to-volume ratio than 300 nm SiNWA. In addition, the variation in SiNWA length also cause the change in the interaction mechanism of acoustic electric effect from mass to elastic effect [20]. In this study, acetone have shown larger frequency shift than other VOC gases toward length of sensing material.

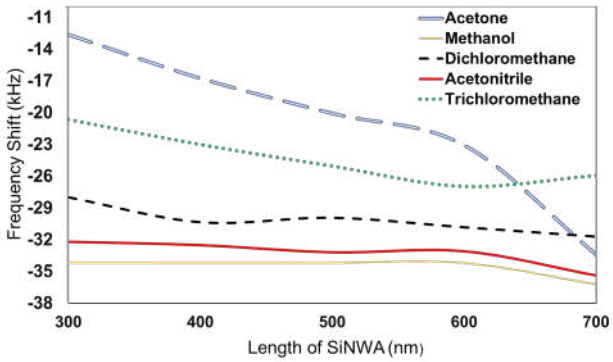

Figure 5 Frequency shift *vs* height of sensing material.

4. CONCLUSION

The SAW-based sensor for detection of diverse gases is promised by means of optimized integration with the sensing layer. A novel SAW gas sensor based on SiNWA was modeled. The sensor response was tested with various VOC concentrations. Due to gas absorption by the sensing layer, the shift resonance frequency increased with increasing VOC gas concentration, allowing for VOC gas detection. The height of SiNWA was then investigated with a resonance frequency shift. The shift of resonance

frequency enhanced as the thickness of SiNWA increased. This is due to the fact that increasing the height of the nanowire array provides a higher surface to ratio. The validation experimentation by fabricating the SiNWA-based SAW sensor has been deferred as part of future work.

ACKNOWLEDGMENT

This work was supported by Ministry of Higher Education Malaysia under the Fundamental Research Grant Scheme (FRGS/1/2018/TK02/UTM/02/25). Mohamed Sultan thank the Universiti Teknologi Malaysia for Industry-International Incentive Grant (IIIG Q.J130000.3651.02M33).

REFERENCES

[1] Zhang, X., et al., "Designed synthesis of Co-doped sponge-like In_2O_3 for highly sensitive detection of acetone gas". *CrystEngComm,* 2019. 21(12): pp. 1876-1885.

[2] Rahman, M.M., M. Alam, and A.M. Asiri, "Fabrication of an acetone sensor based on facile ternary $MnO_2/Gd_2O_3/SnO_2$ nanosheets for environmental safety". *New J Chem*, 2017. 41(18): pp. 9938-9946.

[3] Khan, S.B., et al., "Low-temperature growth of ZnO nanoparticles: photocatalyst and acetone sensor". *Talanta*, 2011. 85(2): pp. 943-949.

[4] Ueta, I., et al., "Breath acetone analysis with miniaturized sample preparation device: In-needle preconcentration and subsequent determination by gas chromatography–mass spectroscopy". *J. Chromatogr. B*, 2009. 877(24): pp. 2551-2556.

[5] Kudo, Y., S. Kino, and Y. Matsuura, "Vacuum Ultraviolet Absorption Spectroscopy Analysis of Breath Acetone Using a Hollow Optical Fiber Gas Cell". *Sensors*, 2021. 21(2), 478.

[6] Rahman, S., et al., "Wireless E-Nose Sensors to Detect Volatile Organic Gases through Multivariate Analysis". *Micromachines*, 2020. 11(6), 597.

[7] Hao, X., et al., "Gas sniffer (YSZ-based electrochemical gas phase sensor) toward acetone detection". *Sensors and Actuators B: Chemical*, 2019. 278: pp. 1-7.

[8] Harathi, N., S. Kavitha, and A. Sarkar, "ZnO nanostructured 2D layered SAW based hydrogen gas sensor with enhanced sensitivity". *Materials Today: Proceedings*, 2020. 33: pp. 2621-2625.

[9] Hoummady, Moussa, Andrew Campitelli, and Wojtek Wlodarski. "Acoustic wave sensors: design, sensing mechanisms and applications." *Smart materials and structures* 6, no. 6 (1997), 647.

[10] Lou, C., et al., "Human Respiratory Monitoring Based on Schottky Resistance Humidity". *Sensors. Materials*, 2020. 13(2), 430.

[11] Feng, P., et al., "Gas sensors based on semiconducting nanowire field-effect transistors. *Sensors*, 2014. 14(9): pp. 17406-17429.

[12] Ghosh, R. and P.K. Giri, "Silicon nanowire heterostructures for advanced energy and environmental applications: a review". *Nanotechnology*, 2016. 28(1), 012001.

[13] Z. Xu and Y. J. Yuan, "Implementation of guiding layers of surface acoustic wave devices: A review," *Biosensors and Bioelectronics,* vol. 99, pp. 500-512, 2018.

[14] Du Plessis, H.G. and W.J. Perold. "Simulation of ZnO enhanced SAW gas sensor". in *Proceed. Comsol Conf.* 2013.

[15] Hasan, M.N., et al., Simulation and fabrication of SAW-based gas sensor with modified surface state of active layer and electrode orientation for enhanced H_2 gas sensing. *Journal of Electronic Materials,* 2017. 46(2): pp. 679-686.

[16] Wang, Wen, et al. "Enhanced sensitivity of a Love Wave-Based methane gas sensor incorporating a Cryptophane-A thin film." *Sensors* 18.10 (2018): pp. 3247.

[17] Moustafa, Mohamed, et al. "Investigation into surface acoustic wave sensor for DCM gas detection using COMSOL multiphysics." *Ferroelectrics* 572.1 (2021): pp. 94-105.

[18] Kirschner, J. Surface Acoustic Wave Sensors (SAWS): Design for Application, Microelectro - mechanical sytems 2010.

[19] Ballantine Jr, D. S., et al. Acoustic wave sensors: theory, design and physico-chemical applications. *Elsevier*, 1996.

[20] Abraham, N., et al., Simulation studies on the responses of ZnO-CuO/CNT nanocomposite based SAW sensor to various volatile organic chemicals. Journal of Science: Advanced Materials and Devices, 2019. 4(1): pp. 125-131